Eur Biophys J (1989) 17:245–255

European Biophysics Journal

The superstructure of chromatin and its condensation mechanism

VI. Electric dichroism and model calculations

M. H. J. Koch[1]*, Z. Sayers[1], A. M. Michon[1], P. Sicre[1], R. Marquet[2], and C. Houssier[2]

[1] European Molecular Biology Laboratory, c/o DESY, Notkestrasse 85, D-2000 Hamburg 52, Federal Republic of Germany
[2] Laboratoire de Chimie Macromoléculaire et Chimie Physique, Sart Tilman (B6), Université de Liège, B-4000 Liège, Belgium

Received February 27, 1989/Accepted in revised form July 27, 1989

Abstract. Electric dichroism and X-ray scattering measurements on solutions of uncondensed and condensed chicken erythrocyte chromatin were interpreted on the basis of model calculations. Information about the state of uncondensed fibers in the conditions of electric dichroism measurements was obtained from scattering patterns recorded as a function of pH, in the presence of spermine and at very low monovalent cation concentrations. Electric dichroism measurements on a complex of uncondensed chromatin with methylene blue were made to determine the contribution of the linker and of the nucleosomes to the total dichroism.

A new approach to calculate the dichroism from realistic structural models, which also yields other structural parameters (radius of gyration, radius of gyration of the cross-section, mass per unit length) was used. Only a restricted range of structures is simultaneously compatible with all experimental results. Further, it is shown that previous interpretations of dichroism measurements on chromatin were in contradiction with X-ray scattering data and failed to take into account the distribution of orientation of the nucleosomes in the fibers. When this is done, it is found that the linker DNA in chicken erythrocyte and sea urchin chromatin must run nearly perpendicularly to the fibre axis. Taken together with the dependence of the fibre diameter on the linker length, these results provide the strongest evidence hitherto available for a model in which the linker crosses the central part of the fibre.

Key words: X-ray solution scattering, synchrotron radiation, electric dichroism, chicken erythrocyte chromatin

Introduction

During the last decade several models have been proposed for the structure of chromatin and the changes it undergoes upon condensation by cations. These models, which are based on the interpretation of observations made with different techniques – mainly electron microscopy and linear dichroism – on chromatin from different sources prepared by different procedures, have been discussed in detail in several recent reviews (Sayers 1988; Butler 1988; Koch 1989). Perhaps not surprisingly, there is no consensus even concerning some of the gross features of these models, such as the mass per unit length (m/l) or the path of the linker DNA. Given the high degree of similarity of the structural components (DNA and histones), some of the differences between models appear, however, to be inconsistencies rather than a reflection of natural variability. In particular, very different values were reported for the electric and flow anisotropy of chromatin at very low ionic strength (McGhee et al. 1980; Sen and Crothers 1986; Dimitrov et al. 1988; Harrington 1985). Recently, the origin of the discrepancies between flow and electric linear dichroism was investigated (Hagmar et al. 1989).

In the present series of papers we have attempted to obtain a model of chicken erythrocyte chromatin and its condensation by cations, that is consistent with the observations from different physical techniques. In this final contribution we show that this model is also consistent with the electric dichroism results and that the differences between dichroism values reported in the literature depend on the detailed experimental conditions. To allow comparison with the latter results, the X-ray solution scattering of long chromatin fragments was obtained in conditions close to those used for dichroism measurements (<5 mM NaCl). Further, the effects of pH on the low order structure and of spermine, which is often used in preparative buffers, on the salt induced condensation were investigated.

Additional constraints on the model were obtained by separating the contribution of the linker and of the core DNA to the dichroism using methylene blue as a

* To whom offprint requests should be sent

probe (Kubista et al. 1985). Interpretation of the results relies on a new approach to calculate the dichroism from realistic structural models that take into account the irregular nature of the system. The parameters used as criteria for acceptance of models of the low order structure are the radius of gyration, the mass per unit length, the radius of gyration of the cross-section, the presence of characteristic bands in the calculated scattering patterns and the values of the reduced dichroism. Only a limited range of sterically allowed conformations simultaneously gives acceptable values of these parameters.

For the condensed fibre, only the maximum contribution of the core DNA to the reduced dichroism can be directly calculated. The results indicate that, in order to satisfy orientation constraints compatible with the X-ray scattering patterns from oriented gels of chicken erythrocyte chromatin (Widom and Klug 1985), the average angle between the linker DNA and the fibre axis must be close to 90° with a standard deviation of 20–40°.

Materials and methods

Preparation of chromatin fragments

Chromatin from chicken erythrocytes was extracted as fragments consisting of 70–90 nucleosomes in TE buffer (5 m*M* *Tris*-HCl, 1 m*M* EDTA, 0.5 m*M* phenylmethylsulfonyl fluoride (PMSF), pH 7.5) following procedures described earlier (Bordas et al. 1986). For salt dependence experiments the samples were dialysed against *Tris* buffer (5 m*M* *Tris*-HCl, 0.5 m*M* PMSF, pH 7.5). Chromatin concentrations were measured by absorption at 260 (1 mg/ml chromatin = 0.52 mg DNA/ml: $A_{260} = 10.4$) and at 310 nm for turbidity correction using a Kontron (UVIKON 810) spectrophotometer. Unless otherwise stated all preparations were carried out at 4 °C.

pH dependence of the structure

Samples containing chromatin ($A_{260} = 70$) in TE buffer were dialysed against *Tris* buffers at pH 4.5, 5.3, 5.8, 6.3, 6.9, 7.3, 7.8, 8.2, 8.6 and used directly for X-ray measurements.

Effect of spermine

A sample of chromatin prepared in TE buffer was first dialysed for 1 h against *Tris* buffer containing 0.2 m*M* spermine and then for 20 h against several changes of *Tris* buffer. In other experiments the sample was dialysed against *Tris* buffer containing 50 m*M* NaCl and then against *Tris* buffer. The material was centrifuged for 15 min at 23,500 *g* and the supernatant was mixed at a final concentration of 3 mg DNA/ml with different amounts of NaCl (60 m*M*) stock solution and measured directly. Control experiments were done using chromatin from the same preparation dialysed against Tris buffer only.

Effect of methylene blue

A stock solution of methylene blue at 2 m*M* in *Tris* buffer was mixed with appropriate amounts of a chromatin solution to obtain a final chromatin concentration of 3 mg DNA/ml and a ratio of dye per 100 bp in the range 0–20. After 1 h the samples were centrifuged for 10 min at 6,000 *g* at room temperature and used immediately for X-ray scattering.

X-ray solution scattering

The measurements were made on the double focusing camera X33 (Koch and Bordas 1983) in HASYLAB on the storage ring DORIS of the Deutsche Elektronen Synchrotron (DESY) using the standard data acquisition and evaluation systems (Boulin et al. 1986, 1988). The mass per unit length (m/l) and the radius of gyration of the cross-section ($R\,x$) were obtained as described earlier (Koch et al. 1988).

Electric dichroism

Chromatin solutions were dialysed against a buffer with 1 m*M* sodium cacodylate, pH 6.5. Dichroism measurements were performed as described by Marquet et al. (1988). Chromatin complexes with methylene blue (MB) were prepared by addition of a concentrated chromatin solution ($A_{260} = 10–20$) to dilute dye solutions ($A_{676} = 0.1$) to a final molar ratio of 0.5–1.0 MB/100 bp. Measurements were made at least 1 h after mixing. A value of $7.5 \times 10^4\ M^{-1}\ cm^{-1}$ was used for the extinction coefficient of methylene blue at a wavelength of 676 nm (Norden and Tjerneld 1982). The small hypochromism of methylene blue resulting from intercalation (Norden and Tjerneld 1982) was taken into account for the determination of the reduced dichroism $\Delta A/A$.

Computer simulations

Uncondensed chromatin. The structure of uncondensed chromatin can be described at low resolution as result-

ing from the convolution of a nucleosome with a jointed chain (Koch 1989). For the calculation of conformations of the jointed chain, the internucleosomal distance (l), the angle between successive links (θ) and the torsion angle involving three successive links (ϕ), were taken to be normally distributed random variables with mean $\langle l\rangle$, $\langle\theta\rangle$ and $\langle\phi\rangle$ and standard deviations $\sigma(l)$, $\sigma(\theta)$ and $\sigma(\phi)$, respectively. Each chain was generated using a random number routine to determine N, usually 50, values of l, θ and ϕ in the appropriate ranges, from which cartesian coordinates were obtained. For each range of variables around [$\langle l\rangle$, $\langle\theta\rangle$, $\langle\phi\rangle$] up to 300 trials were made to find 100 chains in which no contacts between nucleosomes shorter than $d_{\min}$, a value set to 6 or 10 nm, occurred. Results of calculations with a larger number of chains were not significantly different.

For normal distributions of ϕ, values outside the range 0–360° were rejected. This simulates a potential depending on $1+\cos\phi$ classically used to represent hindered rotation. Although calculations were made for the whole range of $\langle\phi\rangle$ only those for $\langle\phi\rangle=180°$ corresponding to zig-zag structures are presented below as they gave the most satisfactory agreement.

Radius of gyration. The radius of gyration (R) was calculated as:

$$R^2=\frac{1}{N}\sum_{i=1}^{N} r_i^2+R_N^2. \tag{1}$$

The first term corresponds to the radius of gyration of a chain of N equal masses with distances r_i from the centre of gravity of the chain. The second term, corresponding to the radius of gyration of the nucleosome is in fact negligible.

Scattering pattern, mass per unit length, radius of gyration of the cross-section of uncondensed chromatin. For each range of geometrical variables (l, θ, ϕ) the average scattering of uncondensed chromatin was evaluated over 100 chains at 250 points in the range $0<s<0.3\ \mathrm{nm}^{-1}$ using Debye's formula (see e.g. Cantor and Schimmel 1980). The scattering factor used was that of the spherically averaged nucleosome calculated from a model where the core histones are represented by 76 spheres of 1.5 nm diameter representing a scattering mass fraction of 0.3. The two turns of DNA superhelix which has a diameter of 9.5 nm and a pitch of 2.7 nm are represented by 32 spheres of 2 nm diameter but corresponding to a scattering mass fraction of 0.7. This model, illustrated elsewhere (Koch 1989), incorporates the main features of the crystallographic structure (Richmond et al. 1984) and gives a radius of gyration (Rg) of 3.8 nm for the complete particle, 4.9 nm for the DNA and 3.2 nm for the histone core. These values should be compared with the corresponding ones, 3.9 nm at infinite contrast, 4.7 ± 0.2 nm and 3.5 ± 0.2 nm, respectively, obtained by neutron scattering on mononucleosomes (Suau et al. 1977).

Intrinsic dichroism. For each conformation of the chain of N nucleosomes the value of the intrinsic reduced dichroism ($\Delta A/A$) was calculated as:

$$\frac{\Delta A}{A}=x_N\cdot\frac{0.75}{N}\sum_{i=1}^{N}\frac{(3\cos^2\gamma_i-1)}{2}-(1-x_N)\frac{1.5}{N-1}\sum_{i=1}^{N-1}\frac{(3\cos^2\beta_i-1)}{2}, \tag{2}$$

x_N is the weight fraction of the nucleosomal DNA (i.e. 166 bp/212 bp in the case of chicken erythrocyte chromatin), β the angle between the electric field and the direction of the linker segment, assumed to be straight, and γ the angle between the field and the axis of the DNA superhelix. The axis of the DNA superhelix was taken to correspond to the normal to the plane of the linker segments joining at that point in the chain. The direction of the electric field (E) was assumed to correspond to the major axis of the ellipsoid of inertia of the chain. The angles β and γ were determined in the range $[0-\pi]$ from the scalar products $(\mathbf{E}\cdot(\mathbf{x}_{i+1}-\mathbf{x}_i))$ and $(\mathbf{E}\cdot[\mathbf{x}_i\times\mathbf{x}_{i+1}])$. The values of the intrinsic reduced dichroism of the linker DNA (−1.5) and of the nucleosomes (0.75) are those given by McGhee et al. (1980).

Condensed chromatin. The structure of condensed chromatin was simulated as follows. The coordinates of the centres of gravity of the nucleosomes were generated on a cylindrical net using a random number routine with $0<x<2\pi R/d$ and $0<y<10$. R is the radius of the cylindrical net, 11.5 nm in the case of chicken erythrocyte chromatin fibres that have an outer radius of 15 nm. This distorted net allows one to represent the nucleosomes as circles with unit diameter and simplifies checking for overlap.

After scaling ($X=d\cdot x$, $Y=y\cdot D$), where D is the largest dimension of the nucleosome (11 nm) and d its thickness (5.5 nm), and conversion to cartesian coordinates, the model of the nucleosome was placed at each point. This model was given a normally or uniformly distributed random rotation around the dyad axis. In some calculations a random shift in the range $-0.2R-0.2R$ was given to simulate variability in fibre radius. Examples of the resulting model of the fibre, which realistically simulates the distribution of orientation of the nucleosomes as well as the axial ratio of the condensed fibres used in the experiments, are illustrated elsewhere (Koch 1989) together with the corresponding calculated scattering patterns.

Since the path of the linker in condensed chromatin is unknown only the contribution of the

nucleosomes (i.e. the first term in (2)) can be evaluated. The contribution of the linker obtained from the difference between the experimental value of the total dichroism and the contribution of the nucleosomes allows one to calculate the value of β. Note that, for a distribution of angles, the value of $\beta_c = \arccos(\langle\cos^2\beta\rangle^{1/2})$ will, in general, be different from $\langle\beta\rangle$, the average value of the angle between the linker and the fibre axis.

Results

X-ray solution scattering

Scattering pattern at very low ionic strength. As illustrated in Fig. 1 at very low monovalent ion concentrations (*Tris* + Na < 5 m*M*) the interference maximum near $s = 0.05\ \text{nm}^{-1}$ shifts to lower *s*-values. The radius of gyration of the cross-section and the relative m/l, which is proportional to $I(0)_x$ decrease as illustrated in Fig. 2. Extrapolation of $I(0)_x$ to zero monovalent ion concentration (i.e. -1 m*M* on the abscissa of Fig. 2) and comparison with the value of 0.8 nucleosome/11 nm, determined earlier at 5 m*M* monovalent cation concentration (Koch et al. 1987a), yields a value around 0.4 nucleosome/11 nm. Similarly, the value of the radius of gyration of the cross-section extrapolated to zero salt concentration is 6 ± 1 nm. This value is in fact less accurate than indicated because of the inaccuracy in the actual salt concentration. It is important to note that the measurements were made on long chromatin fragments since the apparent radius of gyration of the cross-section also depends on the length distribution as indicated by nuclease digestion experiments (Koch et al. 1987b).

It can be excluded that the observed effects, which are reversible, would be due to histone degradation. The condensation properties of chromatin dialysed against very low ionic strength buffers and the results of electrophoretic analysis of the histones were indistinguishable from those of our usual preparations.

Effect of pH. Within the range $5 < \text{pH} < 8$ there is no significant difference between the values of the radius gyration of the cross-section and m/l as indicated in Fig. 3. Below pH 4.8 the structure is irreversibly denatured, whereas at pH 8.6 there is a small decrease of the relative m/l and a shift of the interference maximum to lower *s*-values.

Effect of spermine. Figure 4 illustrates that chromatin dialyzed against spermine followed by a 20 h dialysis against several changes of *Tris* buffer is partially condensed and that the characteristic internucleosomal interference near $0.05\ \text{nm}^{-1}$ is hardly distinguishable.

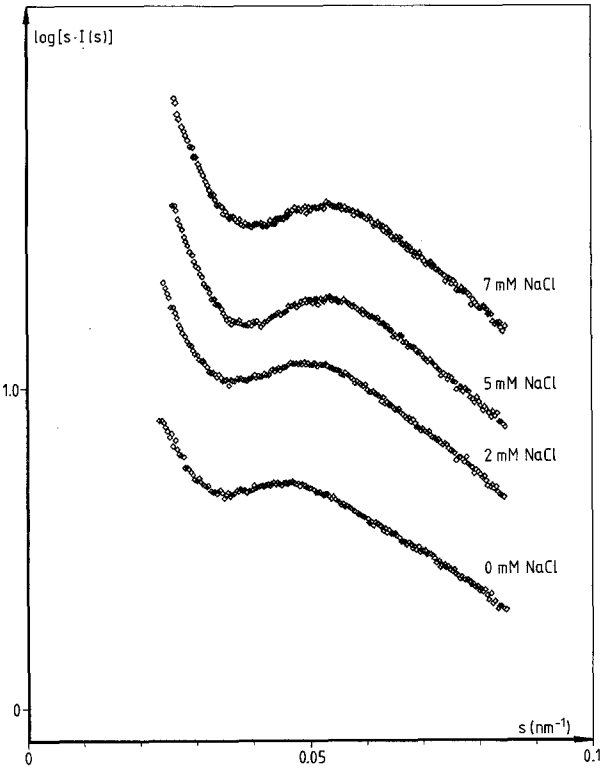

Fig. 1. X-ray solution scattering patterns of chicken erythrocyte chromatin fragments ($A_{260} = 70$) in 1 m*M* *Tris* at increasing NaCl concentrations. Note the shift of the interference maximum to larger *s*-values

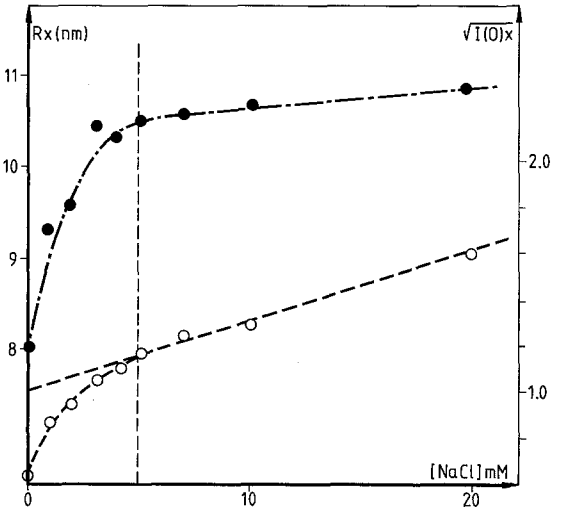

Fig. 2. Cross-section radius of gyration (*Rx*: *full circles*) and relative mass per unit length ($I(0)_x$: *open circles*) of chicken erythrocyte chromatin ($A_{260} = 70$) at very low NaCl concentration. At salt concentrations below the *dashed line* chromatin expands

The scattering patterns for the same sample processed in an identical manner except for the presence of spermine are also shown. Addition of NaCl to concentrations above 5 m*M* leads to the pattern characteristic of condensed chromatin that is observed at NaCl con-

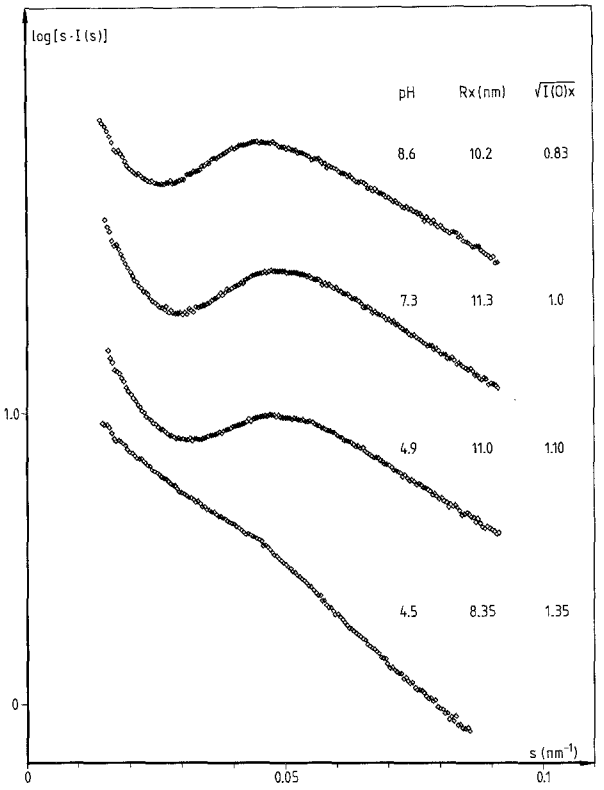

Fig. 3. Solution scattering patterns of chicken erythrocyte chromatin ($A_{260}=70$) at different pH values. R_x is the value of the cross-section radius of gyration and $I(0)_x$ the relative mass per unit length

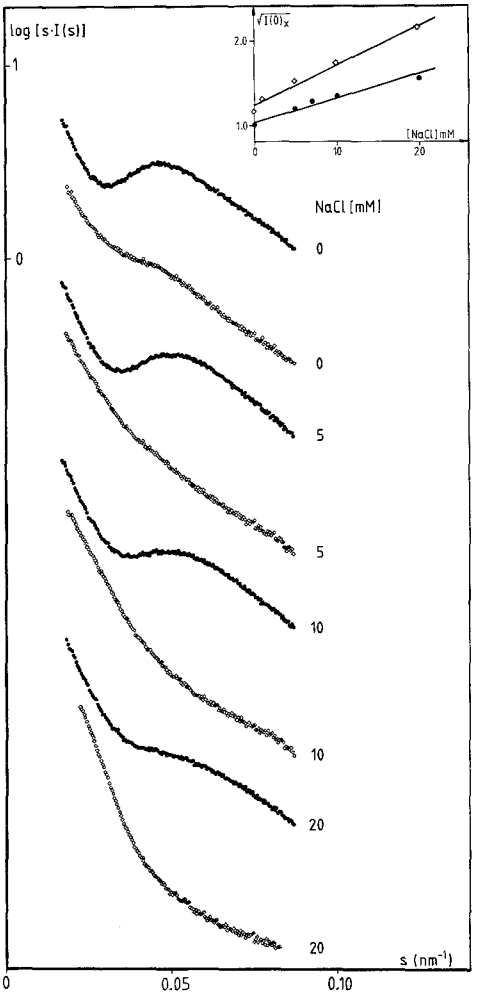

Fig. 4. X-ray solution scattering patterns of chicken erythrocyte chromatin ($A_{260}=60$) dialysed against *Tris* buffer containing 0.2 m*M* spermine (*open diamonds*) followed by dialysis for 20 h against several changes of *Tris* buffer. Patterns from the chromatin from the same preparation dialysed against *Tris* buffer only (*full diamonds*). The *inset* illustrates the increase of the relative mass per unit length with NaCl concentration

centrations above 60 m*M*. The inset in Fig. 4 illustrates the change in relative mass per unit length. Similar results were obtained when the chromatin spermine solution was first dialyzed against *Tris* buffer containing 50 m*M* NaCl and then against *Tris* buffer.

Effect of methylene blue. The influence of methylene blue on the length of the fibre, which is proportional to $I(0)_x^{-1}$, and on the radius of gyration of the cross-section is illustrated in Fig. 5. There is a continuous reduction of the cross-section and of the m/l. At the concentrations of methylene blue (<1 MB/100 bp) used in the electric dichroism experiments no alteration of the chromatin structure is detectable.

Electric dichroism

The use of intercalative dyes such as methylene blue or ethidium bromide is based on the observation that these compounds bind selectively to the linker DNA (Angerer and Moudrianakis 1972; Paoletti et al. 1977; Genest et al. 1981; Kubista et al. 1985). Dichroism at 676 nm in the methylene blue absorption band $\left(\left(\frac{\Delta A}{A}\right)_{676}\right)$ thus reflects the orientation of the linker only. In contrast, the saturation value of the dichroism measured in the DNA absorption band (260 nm) is a weight average of the contribution of the linker DNA $\left(\left(\frac{\Delta A}{A}\right)_L\right)$ and of the chromatosome $\left(\left(\frac{\Delta A}{A}\right)_N\right)$ (see Eq. (2)).

The dependence of the reduced dichroism of chicken erythrocyte chromatin and its MB complexes on the electric field measured at wavelengths of 260 and 676 nm is illustrated in Fig. 6. Distortions of the structure by the electric field, that can usually be detected from the shape of the rise and decay curves or from measurements at various polarization angles of the incident light (Dimitrov et al. 1988; Porschke 1985; Lee et al. 1981; Marquet et al. 1985), were not observed. At the low MB/100 bp ratios used the contri-

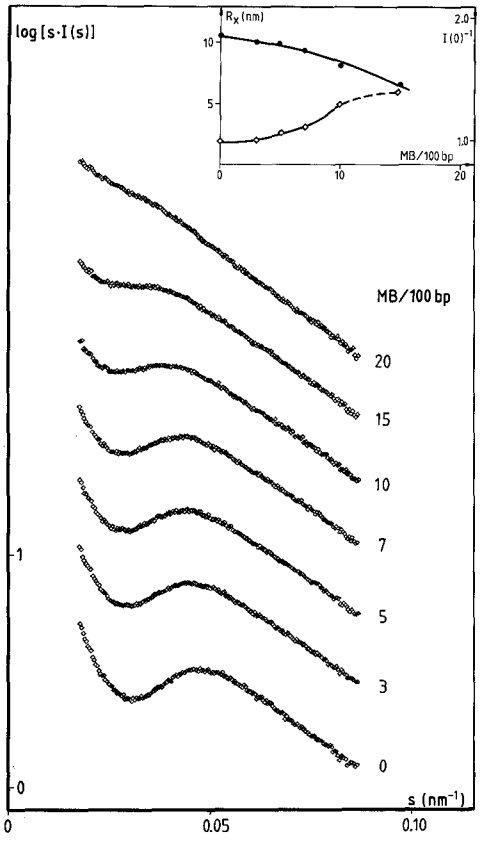

Fig. 5. X-ray solution scattering patterns of chromatin (A_{260} = 60) in the presence of methylene blue (MB) in the range 0–20 MB/100 base pairs (bp). The *inset* illustrates the changes in the radius of gyration of the cross-section (*Rx*: *full circles*) and the relative length ($I(0)^{-1}$: *open circles*) as a function of the number of MB/100 bp

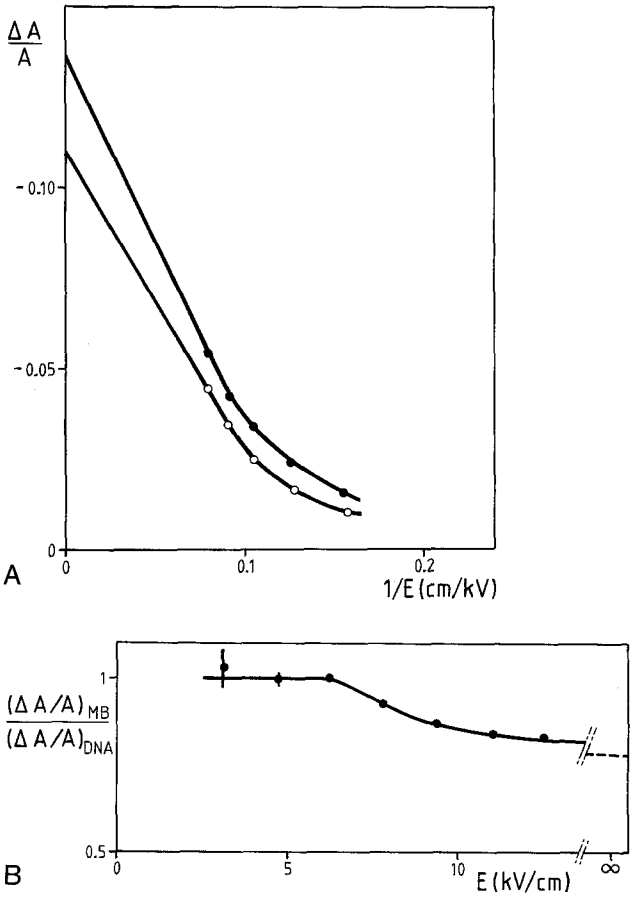

Fig. 6. **A** Dependence of the reduced dichroism at 260 nm (*full circles*) and 676 nm (*open circles*) on the inverse of the electric field for chicken erythrocyte chromatin complexed with methylene blue (1 MB/100 bp) in 1 m*M* sodium cacodylate pH 6.5. **B** ratio between the reduced dichroism of calf thymus DNA at 260 nm and of methylene blue at 676 nm as a function of the electric field

bution of methylene blue to the total absorption at 260 nm is less than 2% and was neglected. Further, in agreement with the X-ray solution scattering data, the structure of chromatin is not significantly perturbed as judged from the unchanged dichroism at 260 nm upon binding of the dye (Kubista et al. 1985; R. Marquet unpublished). Extrapolation to infinite field of the data in Fig. 6A yields $\left(\frac{\Delta A}{A}\right) = -0.135$ in agreement with our previous results (Marquet et al. 1988; Koch et al. 1988) and $\left(\frac{\Delta A}{A}\right)_L = -0.110$. Measurements on calf thymus DNA indicate that the dichroism amplitudes of the DNA bases and of the intercalated dye are identical at field values below 5 kV/cm. As illustrated in Fig. 6B, above 6 kV/cm the dichroism of MB is smaller than that of the DNA bases, probably due to electrochromism (see Fredericq and Houssier 1973). The ratio $(\Delta A/A)^{676}_{MB}/(\Delta A/A)^{260}_{DNA}$ at 12.5 kV/cm is 0.83 and the value of this ratio extrapolated to infinite field is 0.78. It was assumed in the calculation of the intrinsic dichroism that the same effect occurs when MB is bound to chromatin.

One then obtains $\left(\frac{\Delta A}{A}\right)_N = -0.133 \pm 0.025$. Thus, at low ionic strength, the contribution from the chromatosome and from the linker are nearly identical since, after correction for the ratio of the dichroism of MB and DNA at high fields, $\left(\frac{\Delta A}{A}\right)_L = -0.11/0.78 = -0.140 \pm 0.050$. To take into account the fact that the final values depend to some extent on the extrapolation procedure as discussed by McGhee et al. (1980), the errors given here correspond to 2.5 times the calculated standard deviations.

The results of the calculations of the dichroism of uncondensed chromatin and of the contributions of the linker and of the nucleosomes as a function of $\langle\theta\rangle$ and $\sigma(\phi)$ for $\langle\phi\rangle = 180°$ are illustrated in Fig. 7. Only the structures inside the boundaries shown in this map

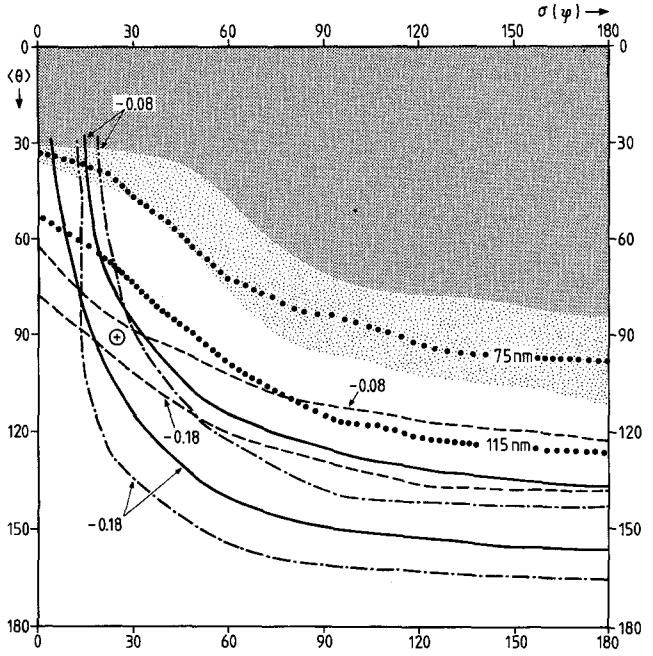

Fig. 7. Results of the computer simulations as a function of $\langle\theta\rangle$ and $\sigma(\phi)$ for $\langle\phi\rangle = 180°$, $\langle l\rangle = 23$ nm, $\sigma(l) = 3$ nm, $\sigma(\theta) = 10°$. The shading indicates the region where more than 50% (*dark*) and 10% (*light*) of the conformations are rejected due to steric hindrance ($d_{min} = 6$ nm). The numbers indicate the values of the contours for the radius of gyration (●●●●), the total dichroism (———), that of the linker (------) and of the nucleosomes (–·–·–). The *cross* indicates the centre of the region where $\left(\frac{\Delta A}{A}\right) = \left(\frac{\Delta A}{A}\right)_L = \left(\frac{\Delta A}{A}\right)_N$

are compatible with the experimental measurements (−0.08 to −0.18).

The calculated values of the contribution of the nucleosomes to the dichroism of condensed chromatin are given in Table 1 together with the contributions of the linker obtained from the experimental values reported by Koch et al. (1988) (0.04) and Sen and Crothers (1986) (−0.1) and the values of $\beta_c = \arccos(\langle\cos^2\beta\rangle^{1/2})$ where β is the angle between the linker and the electric field or fibre axis. Even more negative values of the reduced dichroism of the condensed fibre (−0.2) have been reported by McGhee et al. (1980, 1983). These values have been attributed by Sen and Crothers (1986) to field-induced distortions in the conditions used by McGhee et al. (1980) and are not further considered here.

Radius of gyration

The map in Fig. 7 also illustrates the results of the calculations of the radius of gyration as a function of $\langle\theta\rangle$ and $\sigma(\phi)$ for $\langle\phi\rangle = 180°$ for a chain of 42 nucleosomes. The shading in this map represents regions of steric hindrance. The boundaries indicate the region with radius of gyration values between 75 and 115 nm compatible with the experimental values of Ausio et al. (1984) for fractionated chromatin of approximately the same length in 5 m*M* NaCl ($R = 82$ nm) and 1 m*M* NaCl ($R = 102$ nm).

Table 1. *N:* Calculated contribution of the nucleosomes $(\Delta A/A)_N$ to the dichroism of condensed chromatin and value of arcos $(\langle\cos^2\gamma\rangle^{1/2})$ as a function of $\langle\gamma\rangle$ and $\sigma(\gamma)$. *A:* Contribution of the linker DNA and estimated value of $\beta_c = \arccos(\langle\cos^2\beta\rangle^{1/2})$, the angle between the linker and the fibre axis obtained from the experimental dichroism given by Koch et al. (1988) (0.04). *B:* Corresponding values obtained from the experimental value of Sen and Crothers (1986) (−0.10). The *asterisks* indicate that no value of β_c can be found for this structure

$\sigma(\gamma)^0$	$\langle\gamma\rangle^0$	90		80		70		60		50		40	
0	*N*	−0.374	90	−0.340	80	−0.243	70	−0.094	60	0.090	50	0.285	40
	A	1.603	*	1.475	*	1.107	*	0.544	72	−0.148	51	−0.883	31
	B	0.935	*	0.806	*	0.439	68	−0.124	51	−0.816	33	−1.551	*
10	*N*	−0.340	80	−0.311	76	−0.217	68	−0.079	59	0.104	50	0.280	40
	A	1.475	*	1.365	*	1.012	*	0.477	70	−0.200	49	−0.873	32
	B	0.806	*	0.697	81	0.344	65	−0.176	50	−0.869	32	−1.537	*
20	*N*	−0.259	70	−0.230	68	−0.152	63	−0.032	57	0.125	49	0.259	41
	A	1.169	*	1.059	*	0.744	87	0.310	64	−0.243	48	−0.787	34
	B	0.501	71	0.391	66	0.095	57	−0.358	45	−0.950	30	−1.455	8
30	*N*	−0.147	63	−0.123	61	−0.062	58	0.028	53	0.138	48	0.254	42
	A	0.739	86	0.654	78	0.425	68	0.086	57	−0.329	46	−0.768	35
	B	0.071	57	−0.014	54	−0.239	48	−0.582	40	−0.997	28	−1.432	10
40	*N*	−0.014	56	−0.015	55	0.026	53	0.087	50	0.162	47	0.238	43
	A	0.243	62	0.277	63	0.086	57	−0.138	51	−0.420	44	−0.706	36
	B	−0.429	44	−0.420	44	−0.577	40	−0.806	34	−1.088	25	−1.374	14

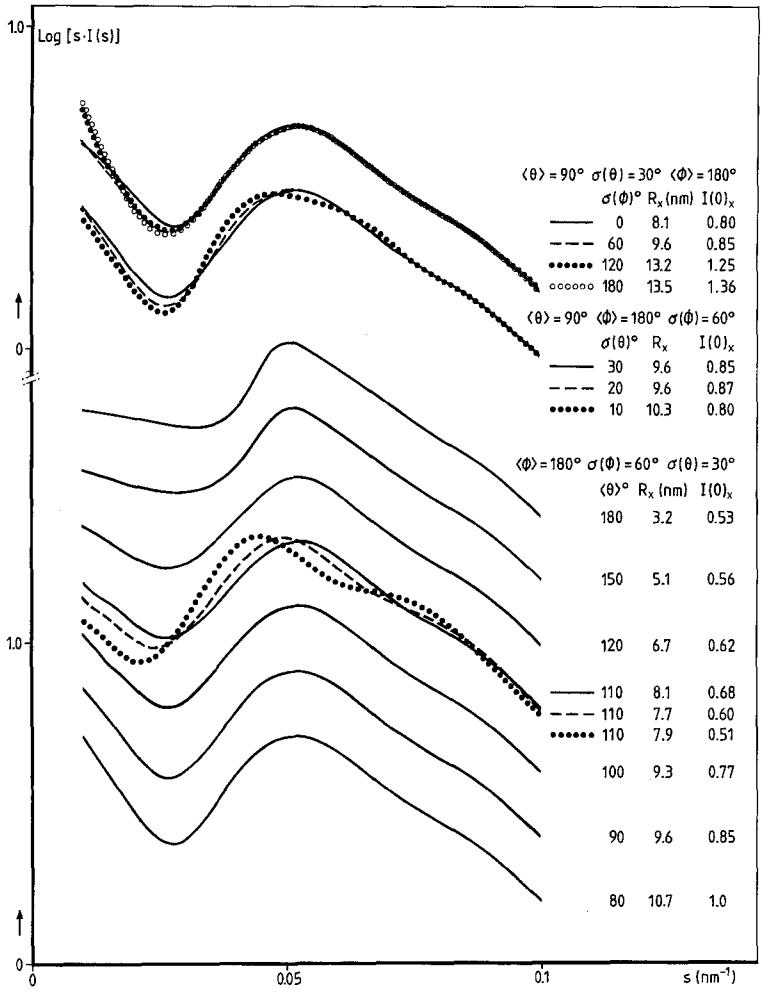

Fig. 8. Scattering patterns for uncondensed chromatin calculated as a function of $\langle\theta\rangle$, $\sigma(\theta)$, $\langle\phi\rangle$ and $\sigma\langle\phi\rangle$, for $\langle l\rangle = 23$ nm, $\sigma(l) = 3$ nm. The superimposed patterns at the top illustrate the influence of $\sigma(\phi)$ and of $\sigma(\theta)$ on the Rx and m/l. The patterns below illustrate the change of shape as a function of $\langle\theta\rangle$. The pattern at $\langle\theta\rangle = 110°$ is also shown for $\langle l\rangle = 25$ nm (-----) and $\langle l\rangle = 28$ nm (●●●●)

Scattering patterns

The scattering patterns for $s < 0.1$ nm^{-1} depend mainly on the relative arrangement of the nucleosomes in the fibers whereas for $s > 0.1$ nm^{-1} they are dominated by the structure of the nucleosomes (Koch 1989). Patterns for a chain of 50 nucleosomes in the range $0 \leqslant s \leqslant 0.1$ nm^{-1} as a function of $\langle\theta\rangle$ for $\langle\phi\rangle = 180°$ are illustrated in Fig. 8. The top curves illustrate that the initial slope, which is related to the radius of gyration of the cross-section increases slightly with $\sigma(\phi)$. When $\langle\theta\rangle$ increases the slope decreases rapidly and the shape of the interference maximum changes. The pattern with $\langle\theta\rangle = 180°$ corresponds to a fully extended 10-nm filament with an interference maximum that has the characteristic shape of a meridional feature. The superimposed patterns for $\langle\theta\rangle = 110°$ illustrate that the interference maximum is shifted to smaller s-values when $\langle l\rangle$ increases.

Discussion

The scattering patterns at salt concentration below 5 mM in Fig. 1 indicate that at vanishing salt concentrations chromatin, like other flexible polyelectrolytes, expands (see Tanford 1961). This approach towards the "10 nm" filament initially observed by Thoma et al. (1979) occurs in a continuous manner. The scattering patterns for uncondensed chromatin in Fig. 8 calculated for increasing average values of the angle θ between successive linker segments and fixed average internucleosomal distance $\langle l\rangle$ correctly reproduce the reduction of the radius of gyration of the cross-section and mass per unit length observed experimentally. If the only modification of the structure were an increase of $\langle\theta\rangle$, the position of the interference maximum would not change much at increasing ionic strength, in contradiction with the observations.

If the simultaneous increase in internucleosomal distance due to straightening of the linker is taken into account, the observed shift towards lower s-values is also reproduced. Elongations of the linker larger than 2–5 nm result in patterns that no longer reproduce the shape of the interference maximum as illustrated in Fig. 8 for $\langle\theta\rangle = 110°$. It can thus be concluded that the mechanism of condensation involves a reduction of $\langle l\rangle$ as well as of $\langle\theta\rangle$.

The measurements as a function of pH prove that the expansion is solely due to the decrease in salt concentration and not to the lower pH resulting from the low buffering capacity of the solutions used for the scattering experiments at very low ionic strengths.

The strong dependence of the structure on ionic conditions below 1 mM monovalent cation concentration explains most of the differences between values reported in the literature since minor changes in buffer composition will lead to large changes in dichroism. Whereas our value of the dichroism (-0.02 at 6 kV) of uncondensed chromatin ($A_{260}=0.5$) is obtained in a buffer containing 1 mM Na^+, the more negative values (-0.15 at 6 kV) of Sen and Crothers (1986) were obtained in a buffer containing 0.5 mM total monovalent cation concentration [M^+] and a low chromatin concentration ($A_{260}=0.2$). Those of McGhee et al. (1980) were obtained at lower monovalent cation concentrations (0.2 mM) and are even more negative (-0.23 at 6 kV).

Evidence for an expansion of the structure is also given by light scattering ($A_{260}=1$), where an increase of the radius of gyration of 20% is observed between 5 and 1 mM monovalent cation concentration (Ausio et al. 1984). Similarly, in electron microscopy, the "10 nm" filaments are only observed below 5 mM monovalent ion concentration (Widom 1986) even at low chromatin concentrations ($0.02<A_{260}<0.2$).

The dialysis experiments with spermine indicate that when spermine is used in the preparative buffers the samples may remain in a semi-condensed state even after prolonged dialysis against very low ionic strength buffers. This may explain the results of Chauvin et al. (1985) and Tjerneld et al. (1982) who found positive anisotropy even at very low ionic strength. The separation of the contribution of the linker and the nucleosomes to the dichroism is justified by the X-ray scattering results on methylene blue intercalation which give unequivocal evidence that at the very low MB concentrations used for the dichroism measurements the structure is not significantly altered in the complex. At sufficiently large concentrations around 3 molecules/100 bp the internucleosomal distance increases and the fibers extend with a concomitant decrease in $R\,x$ and in apparent mass per unit length. This is consistent with earlier experiments on the effect of ethidium bromide intercalation (Bordas et al. 1986).

Figure 9 summarizes the results of the calculations for a disordered zig-zag or helix-like model of uncondensed chromatin. It corresponds to a cut in the map in Fig. 7 at $\sigma(\phi)=60°$. It is clear that only a limited range of values of θ around 80–100° will simultaneously lead to acceptable values of the structural parameters corresponding to the structure at monovalent cation concentrations around 5 mM. Note, that

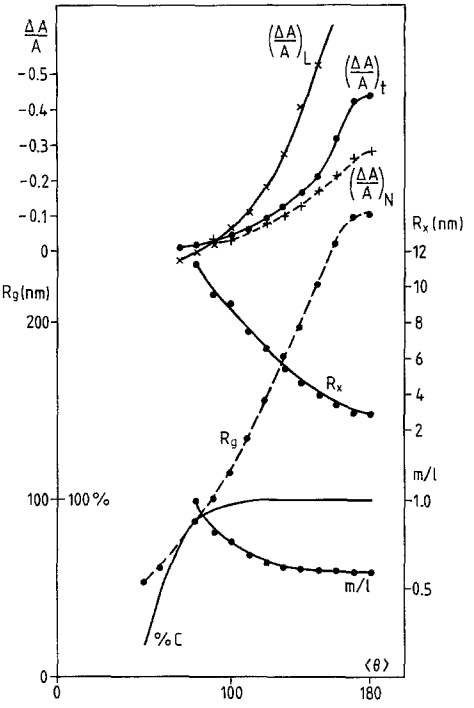

Fig. 9. Summary of the model calculations for uncondensed chromatin as a function of $\langle\theta\rangle$ for $\langle\phi\rangle=180°$ and $\sigma(\phi)=60°$, $\sigma(\theta)=10°$, $\langle l\rangle=23$ nm, $\sigma(l)=3$ nm. Only the region around $\langle\theta\rangle=90°$ simultaneously gives adequate values for all parameters for chicken erythrocyte chromatin at low ionic strength ([M^+] $\simeq 5$ mM). %C: percentage of conformations accepted

the values calculated for the intrinsic dichroism are lower than the experimental values. If one allows for an expansion of the structure resulting from an increase of the value of $\langle\theta\rangle$ of 20–40° a satisfactory agreement with the results at monovalent cation concentrations below 5 mM is also obtained. Owing to the elongation of the linker mentioned above, the variations of $R\,g$, $R\,x$ and m/l are slightly underestimated. The model predicts that the reduced dichroism of chromatin at total monovalent cation concentrations around 5 mM should be very small. This is in agreement with the birefringence results of Chauvin et al. (1985) and the sign inversions ($-$ to $+$) found by flow dichroism on Ehrlich ascite chromatin around 2 mM NaCl (Kubista et al. 1985) and by flow and electric dichroism on chromatin from various sources, including chicken erythrocytes, in the range 1–5 mM NaCl (Dimitrov et al. 1988).

At the field strengths used in our experiments the shape of the signal does not provide any evidence for a distortion of the structure as suggested by Sen and Crothers (1986) on the basis of experiments at fields up to 25 kV/cm.

The calculated values of the dichroism for the model of condensed chromatin in Table 1 indicate that for structures with $\langle\gamma\rangle$ close to 90°, values of the reduced dichroism of the condensed fibres in the range

between −0.10 (Sen and Crothers 1986) and +0.04 (Koch et al. 1988) are only compatible with a rather broad distribution of the orientation of the nucleosomes ($\sigma(\gamma) > 20°$) and, in the case of our measurements, an orientation of the linker nearly perpendicular to the fibre axis.

Models of condensed chromatin with ($\langle\gamma\rangle = 90°$ and $\sigma(\gamma) = 10-30°$) give scattering patterns (Koch 1989) that are in excellent agreement with the experimental solution scattering data and with the diffraction patterns of oriented gels (Widom and Klug 1985). This is important since, in contrast with the structural parameters, the values in Table 1 do not depend much on the fibre diameter but mainly on the distribution of the orientation of the nucleosomes relative to the fibre axis.

The broad distribution of orientation of the nucleosomes also implies that the orientation of the linker corresponds to an angle $\beta_c = \arccos(\langle\cos^2\beta\rangle^{1/2})$ between 60 and 90°. Since the dichroism of the linker can only vary between −1.5 for $\beta = 0$ to +0.75 for $\beta = 90°$ and that of the nucleosomes between +0.75 for $\gamma = 0°$ and −0.375 for $\gamma = 90°$, more ordered structures ($\sigma(\gamma) < 20°$) would require a systematic tilt of the nucleosomes relative to the fibre axis as proposed by Yabuki et al. (1982) or McGhee et al. (1983). The diffraction patterns of oriented fibres (Widom and Klug 1985) give no evidence for such an arrangement of the nucleosomes but Fourier transforms of selected electron micrographs of individual fibers have been interpreted as indicating a tilt of the nucleosomes (Williams et al. 1986).

Experimental values of γ (Sen et al. 1986) correspond to $\arccos(\langle\cos^2\gamma\rangle^{1/2})$. As illustrated in Table 1 for each distribution, in an irregular system these values are not directly related to $\langle\gamma\rangle$ but also depend on the width of the angular distribution. The same applies of course to the experimental values of β as well as to the values of β_c given in Table 1. This allows to interpret the values of the intrinsic dichroism of the linker DNA and the nucleosomes for condensed chromatin from different sources obtained by Sen et al. (1986) in terms of the degree of order in these fibres. Assuming that $\langle\gamma\rangle = 90°$ in all cases, one concludes that fibres of sea urchin chromatin $\left(\left(\frac{\Delta A}{A}\right)_N = -0.32\right.$ and $\left.\left(\frac{\Delta A}{A}\right)_L = +0.29\right)$ are more ordered than those from HeLa $\left(\left(\frac{\Delta A}{A}\right)_N = -0.16\right.$ and $\left.\left(\frac{\Delta A}{A}\right)_L = +0.20\right)$ and calf thymus chromatin $\left(\left(\frac{\Delta A}{A}\right)_N = -0.04\right.$ and $\left.\left(\frac{\Delta A}{A}\right)_L = -0.36\right)$. These values are compatible with $\langle\gamma\rangle = \langle\beta\rangle = 90°$ if one assumes $\sigma(\gamma) = 15°$, $\sigma(\beta) = 30°$ for sea urchin chromatin, $\sigma(\beta) = \sigma(\gamma) = 30°$ for HeLa and $\sigma(\gamma) = 37°$, $\sigma(\beta) = 60°$ for calf thymus chromatin. This leads to the conclusion that in compact fibres like those of sea urchin or chicken erythrocyte chromatin the linker DNA runs nearly perpendicularly to the fibre axis.

Our results confirm that the salt-induced compaction of chromatin is a continuous process over the whole range of ionic strength, with an expansion of the structure at salt concentrations below about 5 m*M*. This expansion does not correspond to a structural transition characteristic of chromatin but to a general property of polyelectrolytes at very low counterion concentrations. The process of compaction, which is characteristic of chromatin, is accompanied by a competitive process of aggregation that can be prevented by an appropriate choice of buffer (e.g. addition of neutral amino acids (see Buche et al. (1989) and references therein). The model calculations show that when this expansion is taken into account, consistent values for the dichroism and for the structural parameters extrapolated to vanishing salt concentration are obtained. The major source of differences in the values of the dichroism of uncondensed chromatin reported by different laboratories lies in the ionic conditions used for the measurements and in the composition of the buffers (e.g. presence of polyamines).

The dichroism of chicken erythrocyte chromatin at salt concentrations around 5 m*M* is close to zero and does not depend much on the degree of condensation in agreement with the observations of Kubista et al. (1985) and Dimitrov et al. (1988).

Interpretation of the dichroism data for condensed chromatin in terms of the orientation of the nucleosomes as well as the degree of order in the fibres allows one to solve the difficulties encountered with interpretations based on variants (Butler 1984; Sen et al. 1986) of the solenoid model originally proposed by Finch and Klug (1976). Integration of these results with structural observations including the dependence of the fibre diameter on the linker length (Williams et al. 1986; Koch et al. 1988) gives the strongest evidence hitherto available for a model of condensed chromatin in which the linker runs across the central part of the fibre and, in cases like chicken erythrocyte and sea urchin chromatin, nearly perpendicularly to the fibre axis.

Acknowledgements. R. M. was supported by a fellowship from the Federation of European Biochemical Societies (FEBS). The Laboratory of macromolecular and physical chemistry in Liège received the support of the Services de Programmation de la Politique Scientifique (ARC contract n° 80/85-90).

References

Angerer LM, Moudrianakis EN (1972) Interaction of ethidium bromide with whole and selectively deproteinized deoxynucleoproteins from calf thymus. J Mol Biol 63:505–521

Ausio J, Borochov N, Seger D, Eisenberg H (1984) Interaction of chromatin with NaCl and $MgCl_2$: Solubility and binding studies, transition to and characterization of the higher order structure. J Mol Biol 177:373–398

Bordas J, Perez-Grau L, Koch MHJ, Nave C, Vega MC (1986) The superstructure of chromatin and its condensation mechanism. I: Synchrotron radiation X-ray scattering results. Eur Biophys J 13:157–174

Boulin C, Kempf R, Koch MHJ, McLaughlin SM (1986) Data appraisal, evaluation and display for synchrotron radiation experiments: hardware and software. Nucl Instrum Methods A249:399–407

Boulin CJ, Kempf R, Gabriel A, Koch MHJ (1988) Data acquisition systems for linear and area X-ray detectors using delay line readout. Nucl Instrum Methods A269:312–320

Buche A, Ouassaidi A, Hacha R, Delpire E, Gilles R, Houssier C (1989) Glycine and other amino-organic compounds prevent chromatin precipitation at physiological ionic strength. FEBS Lett 247:367–370

Butler PJG (1984) A defined structure of the 30-nm chromatin fibre which accommodates different nucleosomal repeat lengths. EMBO J 3:2599–2604

Butler PJG (1988) The organization of the chromatin fibre. In: Adolph KW (ed) Chromosomes and chromatin, I. CRC Press, Boca Raton, pp 57–82

Cantor CR, Schimmel PR (1980). Biophysical chemistry. Freeman, San Francisco

Chauvin F, Roux B, Marion C (1985) Higher order structure of chromatin: influence of ionic strength and proteolytic digestion on the birefringence properties of polynucleosomal fibres. J Biomol Struct Dyn 2:805–819

Dimitrov SI, Smirnov IV, Makarov VL (1988) Optical anisotropy of chromatin: Flow linear dichroism and electric dichroism studies. J Biomol Struct Dyn 5:1135–1148

Finch JT, Klug A (1976) Solenoidal model for superstructure in chromatin. Proc Natl Acad Sci USA 73:1897–1901

Fredericq E, Houssier C (1973) Electric dichroism and electric birefringence. Clarendon Press, Oxford

Genest D, Sabeur G, Wahl P, Auchet J-C (1981) Fluorescence anisotropy decay of ethidium bound to chromatin. Biophys Chem 13:77–87

Hagmar P, Marquet R, Colson P, Kubista M, Nielsen P, Norden B, Houssier C (1989) Electric flow and linear dichroism of unfolded and condensed chromatin: A comparative study at low and intermediate ionic strength. J Biomol Struct Dyn 7:19–27

Harrington RE (1985) Optical model studies of the salt induced 10–30-nm fiber transition in chromatin. Biochemistry 24: 2011–2021

Koch MHJ (1989) Structure and condensation of chromatin. In: Saenger W, Heinemann U (eds) Protein – Nucleic acid interactions. McMillan, London, pp 163–204

Koch MHJ, Bordas J (1983) X-ray diffraction and scattering on disordered systems using synchrotron radiation. Nucl Instrum Methods 208:461–469

Koch MHJ, Vega MC, Sayers Z, Michon AM (1987a) The superstructure of chromatin and its condensation mechanism. III: Effect of monovalent and divalent cations X-ray solution scattering and hydrodynamic studies. Eur Biophys J 14:307–319

Koch MHJ, Sayers Z, Vega MC, Michon AM (1987b) The superstructure of chromatin and its condensation mechanism. IV: Enzymatic digestion, thermal denaturation, effect of netropsin and distamycin. Eur Biophys J 15:133–140

Koch MHJ, Sayers Z, Michon AM, Marquet R, Houssier C, Willführ J (1988) The superstructure of chromatin and its condensation mechanism. V: Effect of linker length, condensation by multivalent cations, solubility and electric dichroism properties. Eur Biophys J 16:177–185

Kubista M, Hard T, Nielsen PE, Norden B (1985) Structural transitions of chromatin at low salt concentrations: A flow linear dichroism study. Biochemistry 24:6336–6342

Lee KS, Mandelkern M, Crothers DM (1981) Solution structural studies of chromatin fibers. Biochemistry 20:1438–1445

McGhee JD, Rau DC, Charney E, Felsenfeld G (1980) Orientation of the nucleosome within the higher order structure of chromatin. Cell 22:87–96

McGhee JD, Nickol JM, Felsenfeld G, Rau DC (1983) Higher order structure of chromatin, orientation of nucleosomes within the 30 nm chromatin solenoid is independent of species and spacer length. Cell 33:831–841

Marquet R, Houssier C, Fredericq E (1985) An electro-optical study of the mechanisms of DNA condensation induced by spermine. Biochim Biophys Acta 825:365–374

Marquet R, Colson P, Matton AM, Houssier C, Thiry M, Goessens G (1988) Comparative study of the condensation of chicken erythrocyte and calf thymus chromatins by di- and multivalent cations. J Biomol Struct Dyn 5:839–857

Norden B, Tjerneld F (1982) Structure of methylene blue DNA complexes studied by linear and circular dichroism spectroscopy. Biopolymers 21:1713–1734

Paoletti J, Magee BB, Magee PT (1977) The structure of chromatin: interaction of ethidium bromide with native and denatured chromatin. Biochemistry 16:351–357

Porschke D (1985) Short electric field pulses convert DNA from "condensed" to "free" conformation. Biopolymers 23:4821–4828

Richmond TJ, Finch JT, Rushton B, Rhodes D, Klug A (1984) Structure of the nucleosome core particle at 7 Å resolution. Nature 311:532–537

Sayers Z (1988) Synchrotron X-ray scattering studies of the chromatin fibre structure. In: Mandelkow E (ed) Synchrotron radiation in chemistry and biology I. Topics in Current Chemistry, vol 145. Springer, Berlin Heidelberg New York, pp 203–232

Sen D, Crothers DM (1986) Condensation of chromatin: Role of multivalent cations. Biochemistry 25:1495–1503

Sen D, Mitra S, Crothers DM (1986) Higher order structure of chromatin: Evidence of photochemically detected linear dichroism. Biochemistry 25:3441–3447

Suau P, Kneale GG, Braddock GW, Baldwin JP, Bradbury EM (1977) A low resolution model for the chromatin core particle by neutron scattering. Nucleic Acids Res 4:3769–3786

Tanford C (1961) Physical chemistry of macromolecules. Wiley, New York

Thoma F, Koller T, Klug A (1979) Involvement of histone H1 in the organization of the nucleosome and of the salt dependent superstructures of chromatin. J Cell Biol 83:403–407

Tjerneld F, Norden B, Wallin H (1982) Chromatin structure studied by linear dichroism at different salt concentrations. Biopolymers 21:343–358

Widom J (1986) Physicochemical studies of the folding of the 100 Å nucleosome filament into the 300 Å filament. J Mol Biol 190:411–424

Widom J, Klug A (1985) Structure of the 300 Å filament: X-ray diffraction from oriented samples. Cell 43:207–213

Williams SP, Athey BD, Muglia LJ, Schappe R, Gough AJ, Langmore JP (1986) Chromatin fibres are left-handed double helices with diameter and mass per unit length that depend on linker length. Biophys J 49:233–250

Yabuki H, Dattagupta N, Crothers DM (1982) Orientation of nucleosomes in the thirty-nanometer chromatin fiber. Biochemistry 21:5015–5020